Available online at www.sciencedirect.com
ScienceDirect
International Journal of Heat and Fluid Flow 27 (2006) 1061–1068
International Journal of HEAT AND FLUID FLOW
www.elsevier.com/locate/ijhff

Sensitivity analysis of freestream turbulence parameters on stagnation region heat transfer using a neural network

Babak Seyedan [a], Chan Y. Ching [b,*]

[a] Hatch Acres, 1235 North Service Road West, Oakville, Ont., Canada L6M 2W2
[b] Department of Mechanical Engineering, McMaster University, Hamilton, Ont., Canada L8S 4L7

Received 12 February 2005; accepted 8 January 2006
Available online 15 March 2006

Abstract

A neural network has been used to predict stagnation region heat transfer in the presence of freestream turbulence. The neural network was trained using data from an experimental study to investigate the influence of freestream turbulence on stagnation region heat transfer. The integral length scale, Reynolds number, all three components of velocity fluctuations and the vorticity field were used to characterize the freestream turbulence. The neural network is able to predict 50% of the test data within ±1%, while the maximum error of any data point is under 3%. A sensitivity analysis of the freestream turbulence parameters on stagnation region heat transfer was performed using the trained neural network. The integral length scale is found to have the least influence on the stagnation line heat transfer, while the normal and spanwise turbulence intensities have the highest influence.

Keywords: Stagnation region heat transfer; Neural network; Sensitivity analysis

1. Introduction

Stagnation region heat transfer is important in many engineering applications. For example, heat transfer from the combustion gases to the turbine blades in a gas turbine is highest in the stagnation region. Accurate predictions of heat transfer in this region are essential to improve the design of blade cooling systems. However, accurate estimation of the stagnation region heat transfer on turbine blades is difficult due to the complexity of the flow field (Maciejewski and Moffat, 1962; Larsson, 1997; Guo et al., 1998). There have been several experimental studies on the effect of freestream turbulence on stagnation region heat transfer, and correlations between the stagnation region heat transfer and the characteristics of freestream turbulence such as turbulent intensity (u'), integral length scale (λ_x) and Reynolds number (Re_D) have been developed (Lowery and Vachon, 1975; Mehendale et al., 1991; Van-Fossen et al., 1995). In most cases, however, the correlations are experiment specific since the heat transfer is not only dependent on the turbulence parameters u', λ_x and Re_D, but also on the distinct nature of the turbulence. For example, the combustion gases exiting the combustor tend to be highly anisotropic and well laced with distinct coherent vortical structures. Hence, for more accurate predictions, the correlation models must take into account the distinct nature of the turbulence. This can be achieved by incorporating the rms of all three components of velocity fluctuations (u', v', w') and vorticity (ω_y, ω_z) in addition to λ_x (Oo and Ching, 2001, 2002). The increased number of variables, however, makes it more difficult to obtain accurate correlations and to determine the relative importance of the different parameters on the heat transfer. In this instance, it is difficult to perform a parametric study due to the difficulty of changing a single turbulence parameter while keeping the others fixed. For example, changing the turbulence grid size to increase the turbulence intensity also increases the integral length scale.

* Corresponding author. Tel.: +1 905 525 9140x24998; fax: +1 905 572 7944.
E-mail address: chingcy@mcmaster.ca (C.Y. Ching).

0142-727X/$ - see front matter © 2006 Elsevier Inc. All rights reserved.
doi:10.1016/j.ijheatfluidflow.2006.01.005

Nomenclature

d	diameter of a grid-rod	w'	rms of fluctuating velocity component in spanwise Z direction (m/s)
D	diameter of cylindrical leading edge	x	distance downstream of the grid (m)
Fr	Frossling number $(Nu/\sqrt{Re_D})$	λ_x	streamwise integral length scale of turbulence (m)
Re_D	Reynolds number based on D	ω_y	rms of fluctuating vorticity component in spanwise Y direction (1/s)
u'	rms of fluctuating velocity component in streamwise direction (m/s)	ω_z	rms of fluctuating vorticity component in spanwise Z direction (1/s)
U	mean freestream velocity (m/s)		
v'	rms of fluctuating velocity component in spanwise Y direction (parallel to stagnation line) (m/s)		

An alternative to developing a correlation using standard regression analysis is to train a neural network (NN) to predict the stagnation region heat transfer. The advantage of this is that the trained neural network can then be used to perform a sensitivity analysis of the turbulence parameters on stagnation region heat transfer. This is particularly useful as it allows some insight into the physics of the problem, especially when the underlying physical–mathematical model is complicated. Neural networks have been used successfully in many engineering applications and are capable of representing the physical knowledge of complex systems. A neural network extracts knowledge from the data presented to it, where the physical knowledge of the system is contained within the rules of the network.

The objective of this paper is to present a neural network technique to predict stagnation region heat transfer in the presence of freestream turbulence. The neural network was trained using experimental data, and Re_D, λ_x, u', v', w', ω_y and ω_z were used to characterize the freestream turbulence. The trained neural network was then used to perform a sensitivity analysis of the freestream turbulence parameters on the stagnation region heat transfer.

2. Experimental facilities

The experimental data used to train the neural network were obtained using a heat transfer model with a cylindrical leading edge in a low-speed wind tunnel. The test section of the wind tunnel is 1-m × 1-m and 20-m in length, with freestream turbulence levels with no turbulence generating grids less than 0.5% at all flow rates. Freestream turbulence with different characteristics was generated using grids of 2.86 cm, 1.59 cm and 0.95 cm diameter parallel rods. The grids were arranged in two different orientations, perpendicular and parallel to the stagnation line (Fig. 1), to obtain freestream turbulence with different and distinct characteristics. For example, for the perpendicular grid orientation, the vortices in the freestream turbulence would be primarily aligned perpendicular to the stagnation line and be more susceptible to stretching as they pass over the stagnation region. All three components of the fluctuating velocities, integral length scale and the spanwise fluctuating

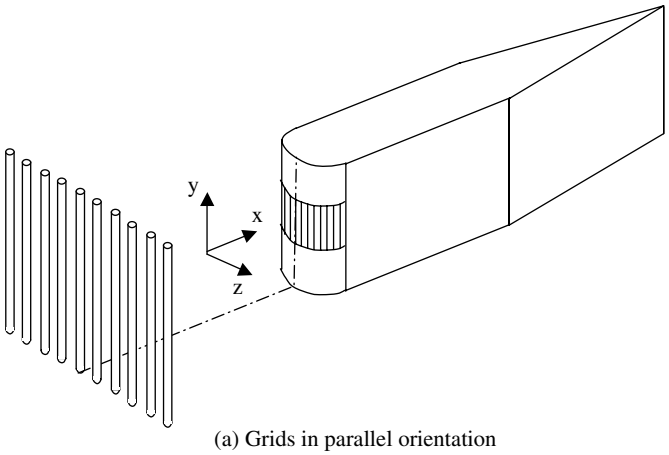

(a) Grids in parallel orientation

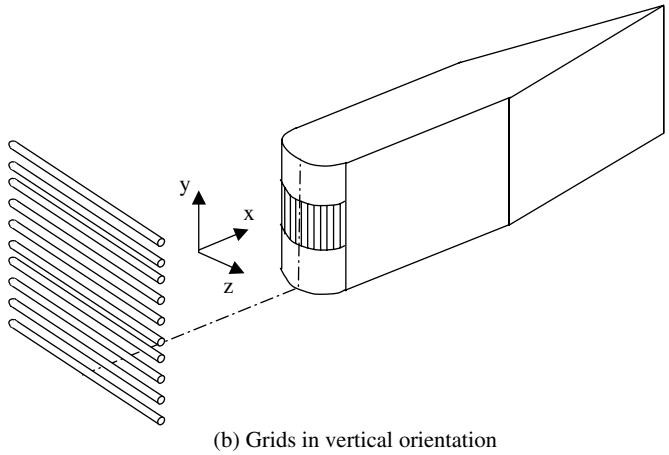

(b) Grids in vertical orientation

Fig. 1. Arrangements of turbulence generating grids.

vorticity components, ω_z and ω_y, were measured using single and X-wires and a vorticity probe. Heat transfer measurements were made with the grids $25d$ to $125d$ upstream of the model at three different Re_D of 67,750, 108,350 and 142,250. The heat transfer model has a cylindrical leading edge of diameter 20.32-cm. A constant heat flux surface is maintained by electrically heating nineteen strips of 0.005-cm-thick stainless steel foil that are evenly

distributed over the stagnation line at the center of the cylindrical leading edge. Each strip is 15.24-cm long, 1.5-cm wide and separated from each other by a gap of 0.1-cm. Six calibrated, 36-gauge T type copper–constantan thermocouples are attached to the underside of every foil strip on one half of the cylindrical leading edge, and are used to estimate the heat transfer along the surface. The complete experimental details and the data reduction procedures are given in Oo and Ching (2002).

3. Experimental results

In this section, only the main heat transfer results at the stagnation line are presented, with the detailed heat transfer results presented and discussed in (Oo and Ching, 2001, 2002). The heat transfer at the stagnation line ($\theta = 0$) with the three grids in perpendicular and parallel orientation are compared with the correlation of VanFossen et al. (1995) in Fig. 2. The correlation was developed for isotropic freestream turbulence generated using square bar mesh grids, and includes Re_D, u' and λ_x. The heat transfer at the stagnation line is presented in terms of the Frossling number ($Fr = Nu/\sqrt{Re_D}$), and is given by

$$Fr = 0.008\sqrt{u' Re_D^{0.8}\left(\frac{\lambda_x}{D}\right)^{-0.574}} + 0.939 \quad (1)$$

For a given rod size, the heat transfer is higher when the rods are aligned perpendicular to the stagnation line, rather than parallel to it. This is likely due to greater vortex stretching of the primary vortices when the grid-rods are in the perpendicular orientation. It has been hypothesized that this is the primary mechanism for the augmentation of stagnation region heat transfer in the presence of freestream turbulence (VanFossen et al., 1995). There is a significant discrepancy between the experimental data and Eq. (1) for the 2.86 cm rod-grid, but the agreement improves with decreasing size of rod. It is speculated that this is due to greater anisotropy of the turbulence with the larger grid-rods. As the size of the grid-rods is decreased, the turbulence generated by the grids become more isotropic and the heat transfer results would agree better with the correlations developed for isotropic turbulence. It is evident from Fig. 1 that correlations developed for isotropic turbulence generated by square mesh grids cannot be reliably used for turbulence with distinct coherent vortical structures. This highlights the necessity for characterizing the turbulence more completely to take into account the distinct characteristics of the freestream turbulence. This can be done, for example, by incorporating u', v', w', ω_y and ω_z in addition λ_x. The increase in the number of turbulence parameters, however, makes it more difficult to obtain accurate correlations using standard regression analysis. A neural network can, in this instance, be trained to predict the stagnation region heat transfer, as it can very easily handle a large number of input variables. A useful feature of a neural network is that it can then be used to perform a sensitivity analysis of the input parameters on the output.

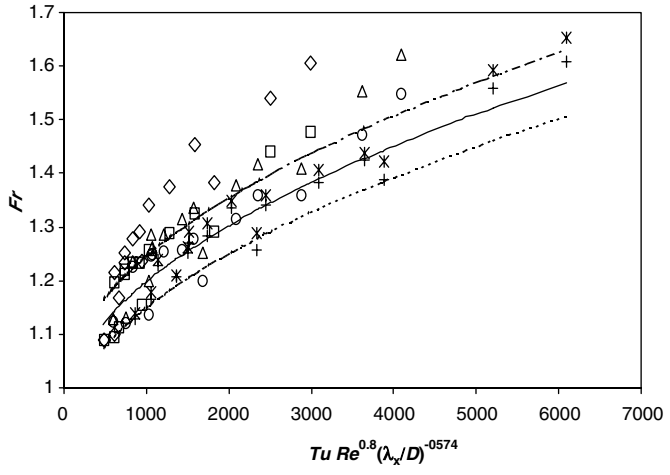

Fig. 2. Stagnation line Fr versus correlation parameter proposed by VanFossen et al. (1995). Perpendicular rod-grids: ◊, 2.86 cm; △, 1.59 cm; ✳, 0.95 cm; parallel rod-grids: □, 2.86 cm; ○, 1.59 cm; +, 0.95 cm; correlation lines: —, VanFossen et al. (1995); – – –, +4%; ---, −4%.

4. Neural network

A neural network (NN) consists of simple processing elements (nodes) linked by weighted connections, and is trained to solve the desired problem. It derives its computing power through a massively distributed structure, and is specified by the net topology, node characteristics and training or learning rules. These rules specify an initial set of weights and indicate how the weights should be updated to improve the performance of the NN. The parallel, multi-parametric character of NNs and their fast computing speeds have permitted neural networks to assert themselves as powerful computational tools in many fields of research and engineering applications. NNs are especially useful where traditional techniques involve long computation times or when the underlying physical–mathematical model is complicated. A NN system, however, requires a certain amount of data, which could be obtained either experimentally or through simulations, for its proper training. In the present investigation, experimental data was used to train a NN to predict the stagnation region heat transfer in the presence of freestream turbulence.

A feed-forward neural network was selected in this instance, due to its simplicity and powerful function approximation capability. The topology of the network in the present study consists of an input layer, one hidden layer and one output layer with an additional bias node, which is often employed as a threshold in the argument of the activation function and whose input always equal unity. There are 7 input neurons, 12 hidden neurons and 1 output neuron in the respective layers. The values of the connection weights are determined through a training procedure. In this case, an error-back propagation algorithm was adopted, which follows from the general

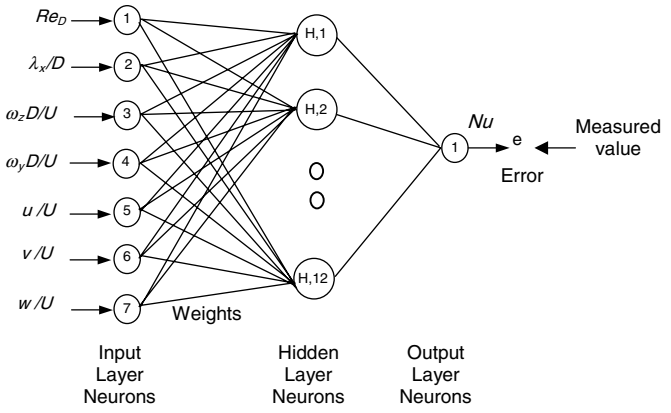

Fig. 3. Schematic of feed-forward artificial neural network.

gradient descent method that minimizes the mean square error between the actual network output and the true value (Muller and Reinhardt, 1991). A schematic of the feed-forward neural network architecture is shown in Fig. 3, where the different turbulence parameters are the input and the heat transfer at the stagnation line, expressed as a Nusselt number Nu, is the desired output.

The input, hidden and output nodes are indicated by n_i, n_h and n_o, respectively, where the signal is processed forward from the input to the output layer. Each node collects the output values, weighted by the connection weights, from all nodes of the preceding layer and processes this information through a sigmoidal function represented as

$$f(x) = 1/(1 + \exp(-x)) \tag{2}$$

A set of n_j inputs and associated n_o outputs are repeatedly presented to the network and the values of the connection weights are modified so as to minimize the average squared output deviation error function, defined as

$$\text{Error} = \sqrt{\frac{1}{2n_p n_o}\sum_{p=1}^{n_p}\sum_{k=1}^{n_o}\left(t_p^k - o_p^k\right)^2} \tag{3}$$

where t_p^k and o_p^k are the true and the neural network computed values of the kth output node, to the pth pattern presented. Through the training, the network is able to build an internal representation of input/output mapping of the problem under investigation. The success of the training strongly depends on the choice of the training parameters, the most crucial being the number of hidden nodes and the learning rate.

The experimental data points were divided into three sets for training, validation and verification. A total of 90 data points were used for training and validating the NN. Once the NN is trained, an independent new blind set of 35 data points is used to verify the performance of the network. The performance of the NN is influenced by the size and efficiency of the training set, by the architecture of the network and by the physical complexity of the problem being solved. It is extremely important to determine the appropriate number of hidden neurons and optimize the learning rate (Muller and Reinhardt, 1991). Hence, a number of trials were performed to determine the optimum number of hidden neurons and learning rate. To obtain the optimum number of hidden neurons, a series of trials was performed where the number of hidden neurons was varied, while keeping the other parameters constant. The effect of the number of hidden neurons on the root mean square error (RMSE) is presented in Fig. 4. The smallest RMSE for the training data set was obtained with 12 hidden neurons, and hereafter for all further computations, 12 hidden neurons were used in the NN. The range of the inputs to NN is listed in Table 1, and the root mean square error defined in Eq. (3), was 0.9% for the training set and 1.1% for the testing set.

The learning rate of the NN was also optimized for the present investigation. The learning algorithm modifies the weights associated with each processing element such that the system minimizes the error between the target output and the actual network output. Fig. 5 shows the influence of the learning parameter on the RMSE. The RMSE is plotted as a function of the number of epochs, a number that represents how many times each data set has been pre-

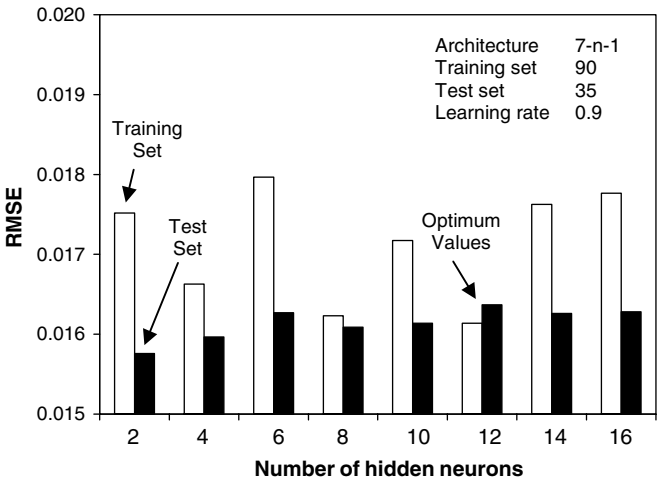

Fig. 4. Optimization of the number of hidden neurons; root mean square error (RMSE) vs. number of hidden neurons.

Table 1
Variation of input and output parameters

#	Variables	Range of variation	
		Minimum	Maximum
Experimental input data			
1	Reynolds number (Re)	67,750	142,250
2	Integral length scale (λ_x/D)	0.0694	0.70
3	Span wise vorticity ($\omega_z D/U$)	4.55	39.50
4	Normal vorticity ($\omega_y D/U$)	4.55	39.50
5	Stream wise turbulence intensity (u'/U)	0.0393	0.1178
6	Normal turbulence intensity (v'/U)	0.0335	0.1233
7	Span wise turbulence intensity (w'/U)	0.0335	0.1233
Experimental measured values			
8	Nusselt number (Nu)	283.4	623.3

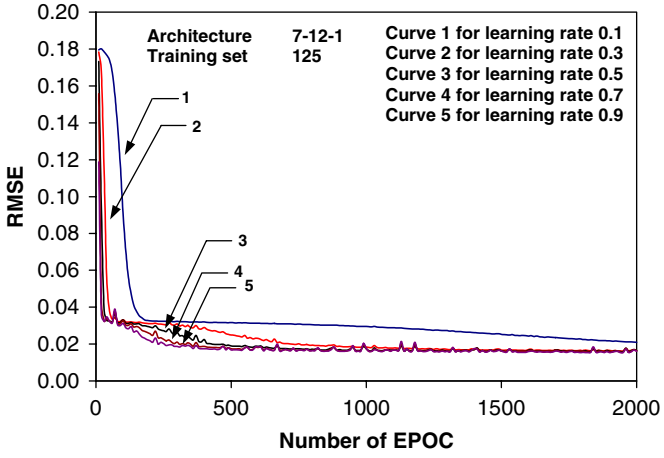

Fig. 5. Optimization of the learning rate value; root mean square error (RMSE) vs. number of EPOC.

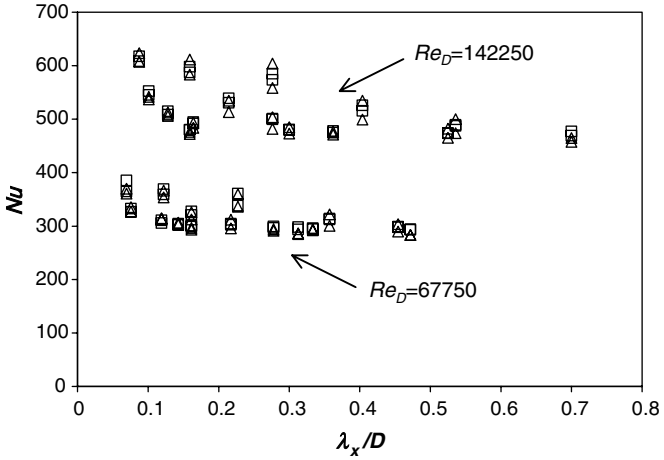

Fig. 6. Variation of Nusselt number (Nu) with integral length scale (λ_x/D). △, Measured values; □, calculated by neural network.

sented to the network. A smaller learning rate parameter results in a smaller change in the network from one iteration to the next and the learning curve is smoother. This is, however, attained at the cost of a slower rate of learning. When the learning rate parameter increases, the learning process is faster. Further, at high epoch sizes, the learning process becomes slower and the curves for learning rates of 0.5, 0.7 and 0.9 are almost the same. The learning rate that, on average, yields a local minimum error with the smallest epoch size is selected as the optimum. A learning rate of 0.9 has been selected for the present NN. The learning is quite rapid and the test error is very close to the training error, which indicates the network is able to generalize the problem well when new test data were presented to it. The training was also carried out for an epoch size of 20,000. The test error and training error was further reduced. The learning process was stopped, when the generalization performance was observed to be satisfactory. Table 2 summarizes the optimal values of the trained NN parameters.

The trained and optimized NN was evaluated using a new set of data points. The error analysis for the cross-validation of the new set of data points showed that the error of the NN output for more than 80% of the data points was below 2%, and the maximum error of any data point was below 3%. This indicates that the network was able to predict the output with a high degree of accuracy for the present problem. To further evaluate the efficacy of the NN, the

Table 2
Neural network optimization configuration

Variable name	Optimization parameter
Number of input neurons	7
Number of hidden neurons	12
Number of output neurons	1
Learning rate	0.9
Number of EPOCs	20000
Training sample size	125
Training error	0.009447
Test error	0.010718

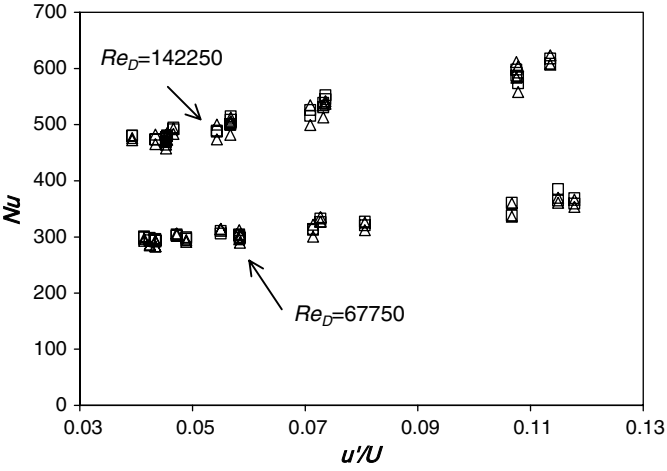

Fig. 7. Variation of Nusselt number (Nu) with streamwise turbulence intensity (u'/U). △, Measured values; □, calculated by neural network.

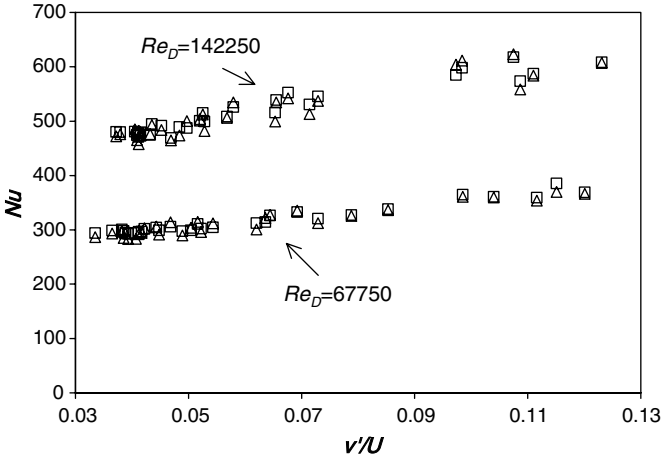

Fig. 8. Variation of Nusselt number (Nu) with normal turbulence intensity (v'/U). △, Measured values; □, calculated by neural network.

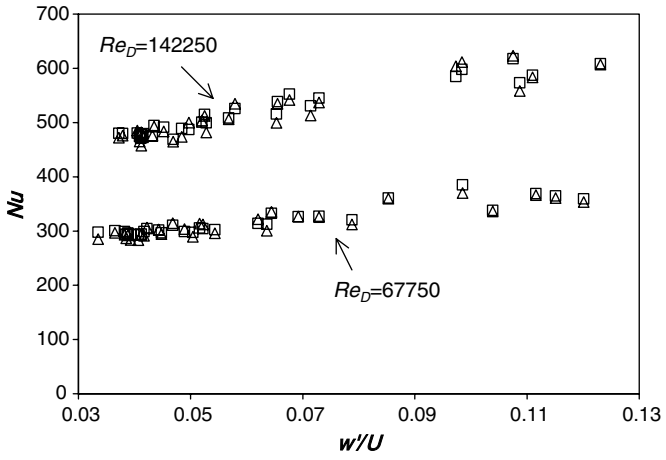

Fig. 9. Variation of Nusselt number (Nu) with spanwise turbulence intensity (w'/U). △, Measured values; □, calculated by neural network.

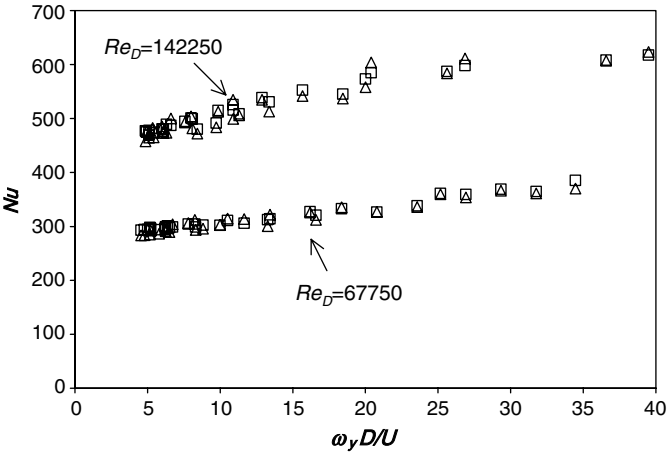

Fig. 10. Variation of Nusselt number (Nu) with normal vorticity ($\omega_y D/U$). △, Measured values; □, calculated by neural network.

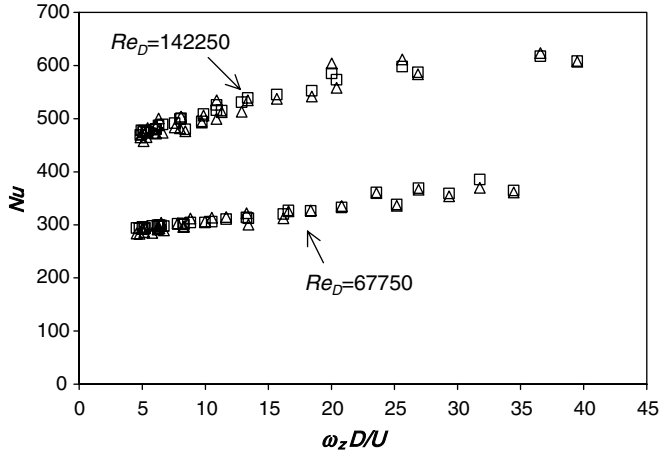

Fig. 11. Variation of Nusselt number (Nu) with spanwise vorticity ($\omega_z D/U$). △, Measured values; □, calculated by neural network.

network was used to predict the variation of the stagnation line heat transfer with the freestream turbulence parameters, and the calculated data are compared to the experimental data in Figs. 6–11. In all cases, there is very good agreement between the heat transfer predicted by the NN and the experimental results. The results indicate that there is a decrease in the heat transfer with an increase in the integral length scale (Fig. 6), and an increase in heat transfer with an increase in the other parameters (Figs. 7–11).

5. Sensitivity analysis

A sensitivity analysis was performed using the trained NN to investigate the relative importance of the different turbulence parameters on the stagnation line heat transfer. This is particularly useful in this instance since the relatively large number of input variables makes the use of standard regression analysis more difficult to implement. The sensitivity analysis yields the gradient of the neural network model response function, and because a neural network model is non-linear, the gradient depends on the point where it is evaluated. Several methods for the sensitivity analysis using neural networks have been presented (Bahbah and Girgis, 1999; Ricotti and Zio, 1999; Neocleous et al., 1999). For example, Bahbah and Girgis (1999) presented a method for the selection of the input parameters, and their ranking of neural network applications in transient stability assessment, and showed that the sensitivity factors converged to stable values. Ricotti and Zio (1999) investigated the dynamic simulation of a steam generator model to point out the difficulties and crucial issues which typically arise when attempting to establish an efficient neural network structure for sensitivity and uncertainty analyses. Neocleous et al. (1999) performed a sensitivity analysis of a neural network model for the estimation of electric load in power plants.

In this study, the sensitivity of the stagnation line heat transfer Nu to the freestream turbulence characteristics λ_x, u', v', w', ω_y, and ω_z are determined using the trained NN. The NN model is represented as

$$y_i = F(x_i) \tag{4}$$

where the output y_i is estimated as a function of the inputs x_i that has p components (i.e. one for each class or output unit). The sensitivity analysis calculates the partial derivative of the output with respect to any of its inputs or the gradient of the NN model $F(x_i)$.

In the present investigation the overall sensitivity is defined as

$$S_j = \sqrt{\frac{\sum_{p=1}^{N}\left(S_p^k\right)^2}{N}} \tag{5}$$

where (S_p^k) is the sensitivity of the NN kth output (o_p^k) to the jth input (I_j^k) for the change of pattern p of (o_p^k) due to the elimination of (I_j^k) and N is the number of patterns in the training set.

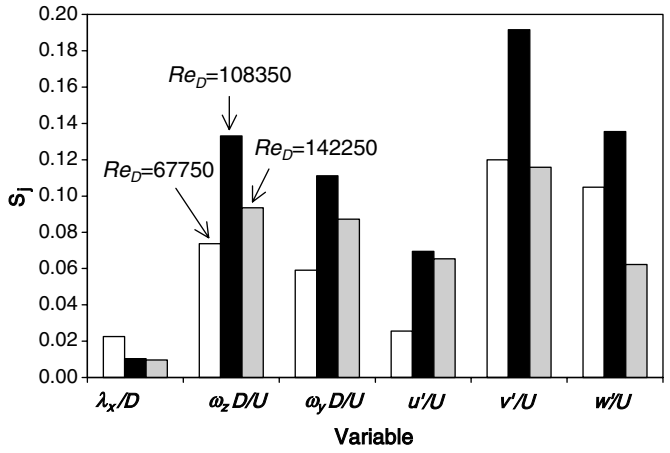

Fig. 12. Overall sensitivity coefficient for the different input variables.

The sensitivity factors (S_j) for each turbulence parameter input (j) corresponding to the three different Reynolds numbers are shown in Fig. 12. The results indicate that the lowest sensitivity factor for all three cases is for λ_x, while the normal turbulence intensity, v', has the highest influence. While there is some effect of the Reynolds number on the sensitivity factors, the trends are very similar. Among the three components of turbulence intensity, u' has the smallest influence. These results are interesting from the point of view that in most studies, u' and λ_x are measured, as these can be easily obtained using a single hot-wire. However, the present analysis shows that these two parameters have the lowest relative influence on the stagnation line heat transfer. For example, at $Re_D = 108{,}350$, the sensitivity of v' on Nu is almost 3 times greater than the sensitivity of u' and 20 times greater than λ_x. The spanwise and normal vorticity components have similar sensitivity factors, and are comparable to that of the spanwise turbulence intensity. These results are in agreement with the hypothesis that the enhancement in the stagnation line heat transfer is due to the vortex stretching of vortices aligned perpendicular to the stagnation line and freestream direction. Vorticity is amplified due to the vortex stretching, and the fluctuating vorticity component of the primary vortices, i.e. ω_z and ω_y for turbulence generated by the rod-grids in perpendicular and parallel orientations, respectively, should play an important role in the stagnation region heat transfer. The products of spanwise vorticity and velocity fluctuating components, $v\omega_z$ and $w\omega_y$, can be interpreted to represent the vortex forces in turbulence, which are analogous to the Coriolis forces (Tennekes and Lumley, 1972). The inclusion of v and w suggest the importance of these two parameters, and these should be included when considering the heat transfer in the stagnation region in the presence of freestream turbulence.

6. Conclusions

A neural network has been developed to predict stagnation region heat transfer in the presence of freestream turbulence. The network was trained using experimental data, and the integral length scale, Reynolds number, all three components of velocity fluctuations and the vorticity field was used to characterize the freestream turbulence. The experiments were performed using a heat transfer model with a cylindrical leading edge in a low speed wind tunnel. The freestream turbulence was generated using a grid of parallel rods, with the rods oriented parallel and normal to the stagnation line. The network consists of one input layer, one hidden layer and one output layer. There are 7 input neurons, 12 hidden neurons and 1 output neuron in the respective layers. The number of hidden neurons and the learning rate of the neural network were optimized to obtain the smallest root mean square error. An error analysis of the validation of the neural network indicate that the error for about 80% of the validation data is below 2%, while the largest error of any point is below 3%. The present work has demonstrated that a neural network can be trained effectively to predict heat transfer using a large number of input variables. A sensitivity analysis has been performed to determine the relative importance of the freestream turbulence characteristics on the stagnation region heat transfer. The results indicate that the normal turbulence intensity has the highest influence, while the integral length scale has the least influence on stagnation region heat transfer. These results are in agreement with the hypothesis that the heat transfer enhancement in the presence of freestream turbulence is due to vortex stretching of the primary vortices aligned normal to the stagnation line and freestream directions.

References

Bahbah, A.G., Girgis, A.A., 1999. Input feature selection for real-time transient stability assessment for artificial neural network (ANN) using ANN sensitivity analysis. IEEE Trans. Neural Network 9, 295–300.

Guo, S.M., Jones, T.V., Lock, G.M., Dancer, S.N., 1998. Computational prediction of heat transfer to gas turbine nozzle guide vanes with roughened surfaces. ASME J. Turbomach. 120, 343–350.

Larsson, J., 1997. Turbine blade heat transfer calculations using two-equation turbulence models. Proc. Instn. Mech. Eng. 221(A), 253–262.

Lowery, G.W., Vachon, R.I., 1975. Effect of turbulence on heat transfer from heated cylinders. Int. J. Heat Mass Transfer 18 (11), 1229–1242.

Maciejewski, P.K., Moffat, R.J., 1962. Heat transfer with very high freestream turbulence: Part I – Experimental data, and Part II – Analysis of results. ASME J. Heat Transfer 114, 827–839.

Mehendale, A.B., Han, J.C., Ou, S., 1991. Influence of high mainstream turbulence on leading edge heat transfer. ASME J. Heat Transfer 113, 843–850.

Muller, B., Reinhardt, J., 1991. Neural Networks – An Introduction. Springer Verlag, New York.

Neocleous, C.C., Papazoglou, T.M., Schizas, C.N., Stratakis, D.I., 1999. Sensitivity analysis of a neural network used for the forecasting of electric power load. Proc. UPEC'99 1, 225–228.

Oo, A.N., Ching, C.Y., 2001. Effect of turbulence with different vortical structures on stagnation region heat transfer. ASME J. Heat Transfer 123, 665–674.

Oo, A.N., Ching, C.Y., 2002. Stagnation line heat transfer augmentation due to freestream vortical structures and vorticity. ASME J. Heat Transfer 124, 583–587.

Ricotti, M.E., Zio, E., 1999. Neural network approach to sensitivity and uncertainty analysis. Reliab. Eng. Syst. Saf. 64, 59–71.

Tennekes, H., Lumley, J.L., 1972. A First Course in Turbulence. The MIT press.

VanFossen, G.J., Simoneau, R.J., Ching, C.Y., 1995. Influence of turbulence parameters, Reynolds number and body shape on stagnation region heat transfer. ASME J. Heat Transfer 117, 597–603.